Research Square

Preprints are preliminary reports that have not undergone peer review.
They should not be considered conclusive, used to inform clinical practice,
or referenced by the media as validated information.

Endogenous Stabilization in Directed Production Networks: An Optimal Control Model with Stochastic Capacity Constraints

Nam Anh Quach

namanhquach27@gmail.com

Hong Bang International University https://orcid.org/0009-0000-7962-6695

Research Article

Keywords: Production networks, Structural growth, Congestion modeling, Infrastructure capacity, Spectral amplification, Stochastic optimal control, Network stability, Transitional dynamics, Computational economics, Middle-income trap

Posted Date: March 3rd, 2026

DOI: https://doi.org/10.21203/rs.3.rs-9002146/v1

License: This work is licensed under a Creative Commons Attribution 4.0 International License.
Read Full License

Additional Declarations: The authors declare no competing interests.

Title

Endogenous Stabilization in Directed Production Networks: An Optimal Control Model with Stochastic Capacity Constraints

Affiliation

Hong Bang International University, School of Mechanics and Technology

Corresponding Author

Nam Anh Quach

Email: namanhquach27@gmail.com

Acknowledgements

The author declares that this research was conducted independently and without external funding. The author thanks the anonymous reviewers and editors for their constructive comments.

Funding Statement

This research received no external funding.

Data Availability

This study does not involve empirical data collection or external datasets. All numerical results are generated from the mathematical model described in the manuscript. No additional data are required.

Declaration of Competing Interests

The author declares no competing financial or non-financial interests.

Endogenous Stabilization in Directed Production Networks: An Optimal Control Model with Stochastic Capacity Constraints

Abstract

This paper develops a stochastic network-control framework for analyzing structural growth transitions in directed production economies subject to congestion constraints. The economy is modeled as a dynamically evolving weighted production network in which inter-firm linkages generate amplification effects, while infrastructure capacity imposes nonlinear attenuation through congestion. The interaction between network propagation and capacity geometry determines an effective amplification index that governs transitional stability. We show that sustained structural upgrading requires keeping amplification below a critical stability threshold. When propagation dominates attenuation, stochastic shocks spread through the network and throughput stagnates. When capacity expansion anticipates network deepening, attenuation dominates propagation, producing a smooth phase transition toward a high-productivity regime. This shift can be summarized by a macroeconomic order parameter capturing the move from amplification-dominated to attenuation-dominated dynamics. Formulated as a finite-horizon stochastic control problem with endogenous network evolution, Monte Carlo simulations confirm the existence of a stabilization threshold and quantify the volatility-reducing role of anticipatory infrastructure expansion.

Keywords: Production networks; Structural growth; Congestion modeling; Infrastructure capacity; Spectral amplification; Stochastic optimal control; Network stability; Transitional dynamics; Computational economics; Middle-income trap

1. Introduction

Structural growth transitions in emerging economies are frequently characterized by a shift from input-driven expansion toward productivity-based development. Classical growth theory, beginning with Robert Solow (1956), formalizes long-run output as a function of capital accumulation and exogenous technological progress. Subsequent endogenous growth models, notably Philippe Aghion and Peter Howitt (1992), emphasize innovation-driven creative destruction as the engine of sustained growth. However, these frameworks typically abstract

from networked production structure and infrastructure-induced frictions that may critically shape transitional dynamics.

Recent advances in production network theory have demonstrated that aggregate fluctuations and growth patterns emerge from micro-level interconnections. Daron Acemoglu, Carvalho, Ozdaglar, and Tahbaz-Salehi (2012) show that sectoral linkages amplify idiosyncratic shocks into aggregate volatility. Similarly, Xavier Gabaix (2011) and David Baqaee and Farhi (2020) establish that nonlinear network interactions can generate large macroeconomic responses even when micro shocks are small. These results underscore that growth and stabilization are fundamentally network phenomena rather than purely representative-agent outcomes.

Yet existing models largely treat infrastructure capacity and policy coordination as exogenous or static constraints. In rapidly developing economies, structural upgrading is frequently accompanied by congestion, capital misallocation, and coordination failures in logistics and production networks. Transportation and congestion economics (e.g., Richard Arnott, de Palma, and Lindsey, 1993; Martin Beckmann, McGuire, and Winsten, 1956) demonstrate how capacity limits generate nonlinear welfare losses and equilibrium distortions. Queueing-theoretic models (Ward Whitt, 2002; Gross et al., 2008) further show that stochastic congestion can induce abrupt regime shifts when utilization approaches critical thresholds.

This paper integrates these strands by modeling the economy as a directed production network subject to stochastic capacity constraints, within a continuous-time stochastic differential game. The framework introduces three strategic actors:

1. A continuum of profit-maximizing firms allocating capital across network nodes;
2. A strategic infrastructure operator determining capacity expansion;
3. A state-level stabilizing agent reallocating capital and coordinating network-wide adjustments.

Unlike standard growth models where policy enters as an exogenous tax or subsidy, the state here is modeled as an endogenous player in a dynamic game, influencing the evolution of network connectivity and congestion. Capital allocation and capacity investment jointly determine the system's feasible production flows, generating a nontrivial dynamic interaction between productivity, congestion, and strategic stabilization.

The model is formulated as a stochastic differential game with Markovian strategies. The equilibrium is characterized by a system of coupled Hamilton–Jacobi–Bellman (HJB) equations (Bellman, 1957; Wendell Fleming & Halil Mete Soner, 2006). We prove the existence of an endogenous stabilization threshold: when infrastructure capacity exceeds a critical level, congestion-induced misallocation disappears and the network converges to a high-productivity regime. Below this threshold, bottlenecks propagate through the directed network, generating persistent output suppression.

By embedding network topology, congestion dynamics, and strategic interaction within a computable HJB framework, the paper contributes a unified model of structural growth transitions driven by capacity geometry and endogenous stabilization.

2. Related Literature and Theoretical Foundations

2.1 Directed Bipartite Production Architecture

To formalize structural growth transitions within a capacity-constrained environment, we represent the economy as a dynamic weighted directed bipartite network

$$G = (U, V, E),$$

where U denotes a set of policy-linked production or financial nodes and V denotes market-oriented firms, including private and foreign-invested entities. The full node set is $N = U \cup V$, with directed edges $E \subset N \times N$ representing input–output dependencies, capital flows, technological spillovers, and credit relationships.

This formulation is consistent with modern production-network theory, which emphasizes that aggregate outcomes emerge from the topology and intensity of intersectoral linkages (Daron Acemoglu et al., 2012; Xavier Gabaix, 2011; David Baqaee & Farhi, 2020). Network structure is encoded in an adjacency matrix $A \in \mathbb{R}^{N \times N}$, where $a_{ij} \geq 0$ measures the dependence of node i on inputs from node j.

Each firm $i \in N$ is characterized by a state vector

$$\mathrm{x}_i(t) \in \mathbb{R}^d,$$

representing capital stock, technological capability, and productive capacity. Aggregate output depends not only on individual states but also on congestion-adjusted network flows.

Unlike representative-agent growth models (Robert Solow, 1956; Philippe Aghion & Peter Howitt, 1992), this structure explicitly embeds interdependence and nonlinear propagation channels, consistent with network science results (Albert-László Barabási, 2016; Mark Newman, 2003).

2.2 Capacity Geometry and Congestion Constraints

Production flows across edges are subject to infrastructure capacity limits. Let $C(t)$ denote aggregate effective capacity supplied by the infrastructure operator. For each edge (i, j), the realized flow $f_{ij}(t)$ satisfies:

$$f_{ij}(t) \leq \phi_{ij}\big(C(t)\big),$$

where $\phi_{ij}(\cdot)$ is an increasing function capturing capacity geometry.

Congestion enters through stochastic queueing dynamics. When utilization approaches capacity, delay variance increases nonlinearly (Whitt, 2002; Gross et al., 2008). This mechanism is consistent with classical congestion models (Richard Arnott et al., 1993; Martin Beckmann et al., 1956), where equilibrium efficiency deteriorates as utilization approaches unity.

Formally, congestion-adjusted productivity of firm $i$is given by:

$$Y_i(t) = F_i\big(\mathrm{x}_i(t), \{f_{ij}(t)\}\big) \cdot \Gamma\big(C(t)\big),$$

where $\Gamma(C)$ is decreasing in expected queue length when capacity is insufficient. This embeds nonlinear regime behavior: as capacity approaches a critical threshold, marginal returns to capital become distorted by congestion externalities.

2.3 Strategic Actors and Differential Game Structure

We model the system as a continuous-time stochastic differential game (Tamer Başar & Olsder, 1999; Avner Friedman, 1971) involving three players:

1. Firms choose capital allocation $u_i(t)$ to maximize discounted profit.
2. Infrastructure Operator chooses capacity investment $v(t)$.

3. State Stabilizer reallocates credit or strategic capital $s_i(t)$.

Capital dynamics follow:

$$d\mathrm{x}_i = [u_i(t) + s_i(t) - \delta \mathrm{x}_i]dt + \sigma_i(\mathrm{x})dW_i(t),$$

where $W_i(t)$ are Brownian motions capturing idiosyncratic shocks.

Infrastructure evolves as:

$$dC = [v(t) - \eta C(t)]dt.$$

Each player solves an interdependent stochastic control problem, and equilibrium is defined as a Markov-perfect Nash equilibrium characterized by coupled Hamilton–Jacobi–Bellman equations (Bellman, 1957; Wendell Fleming & Halil Mete Soner, 2006).

2.4 Hamiltonian Representation of Strategic Capital Dynamics

To analyze stability properties, we introduce a Hamiltonian formulation of the strategic interaction. Let $V^k(\mathrm{x}, C)$ denote the value function of player $k \in \{Firms, Infrastructure, State\}$. The corresponding Hamiltonian for player $k$is:

$$\mathcal{H}^k(\mathrm{x}, C, \nabla V^k) = \max_{control} \left\{ \text{current payoff} + \nabla V^k \cdot \text{state drift} + \frac{1}{2}\mathrm{Tr}(\sigma\sigma^T \nabla^2 V^k) \right\}.$$

Unlike metaphorical physics analogies, this Hamiltonian arises directly from dynamic programming. It captures how marginal value gradients determine optimal capital reallocation and capacity expansion.

The key structural feature is that the state stabilizer's control $s_i(t)$ enters the drift term of all firms simultaneously, effectively reshaping the feasible trajectory space of the network. When capacity C is low, the marginal value of capital becomes distorted by congestion, leading to equilibrium misallocation. As C increases beyond a critical threshold C^*, congestion externalities vanish and the network converges to a high-productivity equilibrium.

2.5 Endogenous Network Formation, Spectral Stability, and the Dual Threshold

A key methodological departure of the present framework is that the production network is not treated as a fixed input–output structure. Instead, the directed adjacency matrix

$$A(t) = \{a_{ij}(t)\}_{i,j=1}^{N} \in \mathbb{R}_{+}^{N\times N}$$

is modeled as an endogenous state variable that co-evolves with firm capacities and infrastructure constraints. This choice is motivated by the production-network literature showing that aggregate outcomes are shaped by the intensity and topology of interdependencies (Acemoglu et al., 2012; Gabaix, 2011; Baqaee & Farhi, 2020), and by network science evidence that resilience properties hinge on topology and link-weight dynamics (Newman, 2003; Barabási, 2016; Gao et al., 2016).

Endogenous link dynamics

Each directed weight $a_{ij}(t)$ captures effective dependence of node i on node j through supply-chain exposure, credit dependence, and technological reliance. We assume $a_{ij}(t)$ follows an Itô diffusion:

$$da_{ij}(t) = b_{ij}\big(t, \mathrm{x}(t), C(t), A(t); s(t)\big)\, dt + \sigma_{ij}\big(t, \mathrm{x}(t), C(t), A(t)\big)\, dZ_{ij}(t),$$

where the drift b_{ij} decomposes into (i) complementarity-driven link formation, (ii) congestion-induced link attenuation, and (iii) strategic stabilization effects. Economically, this captures the fact that link intensities rise when capability complementarities are present (Hidalgo & Hausmann, 2009), but decline when logistics congestion raises effective transaction costs (Arnott et al., 1993; Beckmann et al., 1956) and queue variability degrades reliability (Whitt, 2002; Gross et al., 2008). The stabilizing player's control $s(t)$ enters the drift because directed credit and coordination policies alter the feasibility and attractiveness of specific link formations.

Spectral stability as a macro-network invariant

Let $\lambda_{\max}\big(A(t)\big)$ denote the spectral radius of $A(t)$. In production networks, spectral properties govern propagation and amplification of shocks (Acemoglu et al., 2012) and are closely related to systemic stability and resilience (Gao et al., 2016). In capacity-constrained systems, congestion operates as a topology-dependent "tax" on realized flows; thus, the effective amplification intensity is shaped jointly by $A(t)$ and the capacity state $C(t)$.

We formalize this interaction via an effective amplification index

$$\mathcal{R}(t) \equiv \lambda_{\max}\big(A(t)\big) \cdot \Xi\big(C(t)\big),$$

where $\Xi(C)$ summarizes congestion-induced attenuation of effective throughput, decreasing in C. This representation supports a natural regime classification: when $\mathcal{R}(t) > 1$, link amplification dominates and local disruptions can generate system-wide misallocation; when $\mathcal{R}(t) \leq 1$, propagation is bounded and network-wide stabilization becomes feasible.

Coupling with the finite-horizon differential game

Endogenizing $A(t)$ enlarges the state space to

$$\mathcal{S}(t) = \big(\mathrm{x}(t), C(t), A(t)\big),$$

so each player's value function becomes $V^k(t, \mathcal{S})$ over a high-dimensional state. Under Markovian strategies, equilibrium is characterized by a coupled system of time-dependent HJB equations (Bellman, 1957; Fleming & Soner, 2006), with the network-formation channel entering explicitly through $\nabla_A V^k \cdot b_A$. Intuitively, the marginal value of changing topology is endogenous: it depends on how connectivity affects future congestion, returns to capital, and the ability of the stabilizer to dampen network-wide amplification.

The dual stabilization threshold

The central object is a time-dependent transitional stabilization threshold $C^*(t)$, characterized in two equivalent ways:

1. Spectral characterization (A): $C^*(t)$ is the minimal capacity level such that equilibrium policies ensure $\mathcal{R}(t) \leq 1$ along the equilibrium path, i.e., spectral amplification is dominated by congestion attenuation.

2. Value-function characterization (C): $C^*(t)$ is the minimal capacity level such that the stabilizer's equilibrium value function $V^S(t, \mathcal{S})$ becomes strictly convex in the capital allocation state in the relevant region, eliminating congestion-trap equilibria by restoring marginal incentives for productive reallocation.

Section 4 proves existence and uniqueness of equilibrium value functions as viscosity solutions to the coupled HJB system and then establishes the equivalence of these spectral and value-function thresholds. This yields a mathematically operational definition of "endogenous stabilization" in evolving production networks.

3. Capacity Geometry and Stochastic Transport Constraints

3.1 Infrastructure as a Capacity Geometry Constraint

Standard macroeconomic growth models typically abstract from physical and logistical frictions by assuming frictionless capital mobility and instantaneous adjustment across sectors. While analytically convenient, this assumption is inconsistent with the structural realities of rapidly expanding production networks, where physical throughput constraints and congestion externalities materially affect equilibrium outcomes.

We formalize infrastructure limitations as a capacity geometry constraint imposed on aggregate network throughput.

Let

$$\mathrm{Q}(t) \in \mathbb{R}^m$$

denote the vector of aggregate systemic throughput at time t. Components of $\mathrm{Q}(t)$ represent effective physical and digital flows across network edges, including:

- Export logistics,
- Domestic supply-chain flows,
- Energy transmission,
- Data and communication infrastructure.

These flows are not unconstrained. They must lie within a feasible capacity region:

$$\mathrm{Q}(t) \in \Omega\big(\mathrm{u}(t)\big) \subset \mathbb{R}^m,$$

where $\mathrm{u}(t) \in \mathbb{R}^m$ is the vector of infrastructure investment controls selected by the infrastructure operator.

The set $\Omega(\mathrm{u})$ is assumed to be compact, convex, and increasing in u. Its boundary

$$\partial\Omega(\mathrm{u})$$

represents systemic bottlenecks, including port saturation, rail congestion, grid overload, and bandwidth constraints.

3.2 Stochastic Throughput Dynamics

Throughput evolves as a stochastic process reflecting endogenous expansion and exogenous shocks. We model:

$$d\mathrm{Q}(t) = \left[\Lambda \mathrm{Q}(t) + \Gamma \mathrm{u}(t) - \nabla_{\mathrm{Q}} \Phi\big(\mathrm{Q}(t), \mathrm{u}(t)\big)\right] dt + \Sigma\big(\mathrm{Q}(t)\big) d\mathrm{W}(t),$$

where:

- $\Lambda \in \mathbb{R}^{m \times m}$captures intrinsic network-driven throughput growth (consistent with production network amplification; Acemoglu et al., 2012),
- $\Gamma \in \mathbb{R}^{m \times m}$maps infrastructure investment into effective capacity expansion,
- $\mathrm{W}(t)$is an m-dimensional Wiener process,
- $\Sigma(\mathrm{Q})$captures stochastic volatility from transport delays and global supply shocks.

3.3 Congestion Potential and Friction Gradient

The function

$$\Phi: \mathbb{R}^m \times \mathbb{R}^m \to \mathbb{R}_+$$

is a congestion potential, encoding nonlinear logistical frictions.

We impose:

1. Φ is continuously differentiable in Q.
2. Φ is convex in Q.
3. Divergence at capacity boundary:

$$\lim_{\mathbf{Q} \to \partial \Omega(\mathbf{u})} \Phi(\mathrm{Q}, \mathrm{u}) = +\infty.$$

This condition ensures that as throughput approaches infrastructural limits, marginal congestion cost diverges.

This structure is consistent with:

- Peak-load congestion models (Arnott et al., 1993),

- Wardrop equilibrium under capacity constraints (Beckmann et al., 1956),
- Heavy-traffic queueing asymptotics (Whitt, 2002).

The term

$$\nabla_{\mathrm{Q}}\Phi(\mathrm{Q},\mathrm{u})$$

acts as a friction gradient that endogenously dampens throughput expansion near capacity.

3.4 Integration with Production Network State

Throughput $\mathrm{Q}(t)$links directly to the adjacency matrix $A(t)$ defined in Section 2.

Let the effective network weight satisfy:

$$a_{ij}^{\mathrm{eff}}(t) = a_{ij}(t) \cdot \Xi\big(C(t), \mathrm{Q}(t)\big),$$

where the congestion attenuation function satisfies:

$$\Xi(C, \mathrm{Q}) = \exp\big(-\beta\Phi(\mathrm{Q},\mathrm{u})\big), \beta > 0.$$

Congestion affects not only flows but also the effective topology of the production network.

The spectral radius becomes:

$$\lambda_{\max}^{\mathrm{eff}}(t) = \lambda_{\max}\big(A(t)\big) \cdot \Xi\big(C(t), \mathrm{Q}(t)\big).$$

This directly links capacity geometry to the spectral stabilization condition defined previously.

3.5 Structural Regimes Induced by Capacity Geometry

The interaction between intrinsic growth $\Lambda\mathrm{Q}$ and the friction gradient $\nabla\Phi$ generates two qualitatively distinct regimes.

Regime I: Capacity-Constrained Congestion

If infrastructure investment is insufficient, then:

$$\Lambda\mathrm{Q} > \nabla\Phi(\mathrm{Q},\mathrm{u}),$$

only for small Q. As Q grows, congestion dominates, driving:

$$d\mathrm{Q}(t) \approx 0,$$

implying throughput plateau.

In this regime:

$$\lambda_{\max}^{eff}(t) > 1,$$

and network amplification reinforces misallocation.

Regime II: Stabilized Capacity Expansion

If infrastructure investment expands $\Omega(\mathrm{u})$sufficiently fast, then:

$$\nabla\Phi(\mathrm{Q}, \mathrm{u})$$

remains bounded for all relevant Q, ensuring sustained throughput growth.

In this regime:

$$\lambda_{\max}^{eff}(t) \leq 1,$$

implying bounded propagation and stable structural upgrading.

3.6 Dynamic Role of Infrastructure Control

Unlike static congestion pricing models, infrastructure investment here shifts the feasible region:

$$\Omega\big(\mathrm{u}(t + \Delta t)\big) \supset \Omega\big(\mathrm{u}(t)\big).$$

Thus, the infrastructure operator affects both:

- Current throughput drift $\Gamma\mathrm{u}(t)$,
- Future geometry of the capacity manifold.

This dynamic outward shift of $\partial\Omega(\mathrm{u})$ plays a central role in determining the transitional stabilization threshold $C^*(t)$.

3.7 Compatibility with the HJB Framework

The throughput dynamics augment the state space:

$$\mathcal{S}(t) = \big(\mathbf{x}(t), C(t), A(t), \mathrm{Q}(t)\big).$$

Under standard Lipschitz and growth conditions, the augmented system remains well-posed. The generator of the state process now includes:

$$\nabla_{\mathrm{Q}} V^k \cdot [\Lambda \mathrm{Q} + \Gamma \mathrm{u} - \nabla \Phi] + \frac{1}{2} \mathrm{Tr}\big(\Sigma \Sigma^T D_{\mathrm{Q}}^2 V^k\big).$$

Because Φ diverges at capacity boundaries, the state remains confined to the interior of $\Omega(\mathrm{u})$, ensuring admissibility of the viscosity solution framework.

4. Optimal Stabilization, Viscosity Equilibrium, and the Transitional Threshold

This section integrates the stochastic optimal control structure of the stabilizing agent with the existence, uniqueness, and threshold properties of the finite-horizon differential game. We establish (i) well-posedness of the controlled state system, (ii) viscosity characterization of equilibrium value functions, and (iii) existence and dual characterization of the transitional stabilization threshold.

Throughout, the time horizon is finite: $t \in [0, T]$.

4.1 Well-Posedness of the Controlled State Dynamics

Let the full state vector be:

$$\mathcal{S}(t) = \big(\mathbf{x}(t), C(t), A(t), \mathrm{Q}(t)\big).$$

Assumptions

A1 (Regularity).
All drift and diffusion coefficients are continuous in $(t, \mathcal{S})$, globally Lipschitz in $\mathcal{S}$, and satisfy linear growth conditions.

A2 (Admissible Controls).
Control processes (u, v, s) are progressively measurable and square-integrable.

A3 (Convex Control Costs).
Running payoff is continuous and of polynomial growth; control costs are strictly convex quadratic.

A4 (Congestion Potential).

The congestion potential $\Phi(\mathrm{Q}, \mathrm{u})$ is convex in Q, continuously differentiable, and diverges at $\partial\Omega(\mathrm{u})$.

A5 (Spectral Regularity).

The mapping $A \mapsto \lambda_{\max}(A)$ is locally Lipschitz on the admissible domain.

Proposition 1 (Existence and Uniqueness of State Process)

Under A1–A2, for any admissible strategy profile, the coupled SDE system admits a unique strong solution on $[0, T]$.

Proof.

Standard Itô existence–uniqueness theory applies under global Lipschitz and linear growth conditions. Divergence of Φprevents boundary escape of $\mathrm{Q}(t)$.

4.2 The Stabilizer's Finite-Horizon Control Problem

The stabilizing agent maximizes:

$$V^S(t, \mathcal{S}) = \sup_{s(\cdot)} \mathbb{E}_{t,\mathcal{S}} \left[\int_t^T \left(\sum_{i=1}^N Y_i(\tau) - \frac{\gamma_s}{2} \sum_{i=1}^N \| s_i(\tau) \|^2 \right) d\tau + \Phi^S\big(\mathcal{S}(T)\big) \right].$$

Control $s_i(t)$ affects:

- Capital drift,
- Network evolution,
- Throughput congestion indirectly.

4.3 Dynamic Programming and HJB Characterization

Proposition 2 (Dynamic Programming Principle)

Under A1–A3, the value function satisfies the DPP:

$$V^S(t, \mathcal{S}) = \sup_s \mathbb{E} \left[\int_t^\tau \text{flow payoff} + V^S\big(\tau, \mathcal{S}(\tau)\big) \right].$$

Theorem 1 (Viscosity Solution Characterization)

Under A1–A3, V^S is a viscosity solution to the finite-horizon HJB equation:

$$\frac{\partial V^S}{\partial t} + \sup_s \left\{ \mathcal{L}^{u^*,v^*,s} V^S + \sum_i Y_i - \frac{\gamma_s}{2} \sum_i \| s_i \|^2 \right\} = 0,$$

with terminal condition $V^S(T, \mathcal{S}) = \Phi^S(\mathcal{S})$.

Sketch.
Follows from DPP and standard test-function arguments in viscosity theory.

Theorem 2 (Uniqueness via Comparison)

Under A1–A3, the HJB admits a unique viscosity solution in the class of continuous functions with polynomial growth.

Quadratic control costs yield coercive Hamiltonians, permitting the comparison principle.

4.4 Optimal Routing Policy

Because the Hamiltonian is strictly concave in control, the first-order condition yields:

$$s_i^*(t) = \frac{1}{\gamma_s} \left(\nabla_{\mathbf{x}_i} V^S + \sum\nolimits_j \zeta_{ij} \frac{\partial V^S}{\partial a_{ij}} \right).$$

Stabilization reallocates capital toward nodes with highest marginal value, incorporating both direct productivity and network spillovers.

This formally interprets stabilization as optimal resource routing over an evolving topology.

4.5 Congestion Interaction in the HJB

The throughput drift term contributes:

$$\nabla_{\mathrm{Q}} V^S \cdot [\Lambda \mathrm{Q} + \Gamma \mathrm{u} - \nabla \Phi(\mathrm{Q}, \mathrm{u})].$$

Two mechanisms arise:

1. When congestion is mild, intrinsic growth dominates and marginal throughput expansion increases value.

2. As $\mathrm{Q} \to \partial\Omega(\mathrm{u})$, $\nabla\Phi \to \infty$,
   suppressing marginal value and altering optimal intervention priorities.

The diffusion term:

$$\frac{1}{2}\mathrm{Tr}\left(\Sigma^T D_{\mathrm{Q}}^2 V^S \Sigma\right)$$

penalizes operating near capacity due to volatility amplification.

4.6 Transitional Stabilization Threshold

Define the effective amplification index:

$$\mathcal{R}(t) = \lambda_{\max}\big(A(t)\big)\Xi\big(C(t), \mathrm{Q}(t)\big).$$

Definition (Threshold)

$$C^*(t) = \inf\{C : \exists \text{ equilibrium s.t. } \mathcal{R}(\tau) \leq 1 \ \forall \tau \in [t, T]\}.$$

4.7 Dual Characterization Theorem

Theorem 3 (Spectral–Convexity Equivalence)

Under A1–A5, the following are equivalent:

1. $C(t) \geq C^*(t) \Rightarrow \mathcal{R}(t) \leq 1$ (spectral stabilization).
2. $C(t) \geq C^*(t) \Rightarrow V^S(t, \mathcal{S})$is strictly convex in x (value-function stabilization).

Moreover, $C^*(t)$ is continuous in time and weakly decreasing in $T - t$.

Proof Sketch

i) Spectral → Convexity.
When $\mathscr{R}$(t) ≤ 1, the effective propagation operator

$$\mathcal{A}_{eff}(t) = A(t)\,\Xi(C(t), Q(t))$$

has spectral radius at most unity. By Perron–Frobenius theory for nonnegative matrices, the associated linearized drift mapping is non-expansive in the positive orthant. Combined with convex congestion costs and quadratic control penalties, the Hamiltonian remains strictly

concave in control and jointly convex in the state variables. Standard stability results for viscosity solutions of controlled diffusions then preserve convexity of V_S along equilibrium trajectories.

(ii) Convexity → Spectral Bound.
Suppose instead that $\mathscr{R}(t) > 1$ on a nontrivial interval. Then the linearized network propagation operator admits a dominant eigenvalue strictly larger than one, implying locally increasing returns in the state drift along the Perron eigenvector direction. This induces directional convexity loss in the Hamiltonian through amplification of marginal continuation values. Such amplification violates the comparison principle for convex viscosity solutions with polynomial growth, contradicting strict convexity of V_S. Therefore, convexity of the value function requires $\mathscr{R}(t) \leq 1$.

Continuity of $C^*(t)$ follows from local Lipschitz continuity of the spectral radius with respect to matrix entries and stability of viscosity solutions under continuous parameter perturbations.

5. Computational Simulations and Network Resilience

5.1. Purpose and computational logic

The analytical core of the paper identifies a stabilization mechanism that is inherently networked (through directed inter-firm dependencies) and capacity constrained (through congestion/friction that diverges as throughput approaches infrastructural limits). Consequently, empirical validation cannot be restricted to scalar macro time-series; the mechanism must be exhibited as an emergent property of a co-evolving production network subject to stochastic transport shocks and policy-driven capacity expansion. Following the computational economics tradition—where structural dynamics are validated by numerically integrating a model that is analytically well-posed but not closed-form solvable at macro scale (Judd, 1998; Lucas & Stokey, 1989; Sargent & Stachurski, 2013)—we implement a Monte Carlo simulation that jointly evolves:

1. a directed weighted adjacency $A(t)$ representing input-output / capital-routing channels (Acemoglu et al., 2012; Baqaee & Farhi, 2020),
2. an aggregate throughput state $Q(t)$ (exports + domestic logistics + digital flow proxy),

3. an endogenous capacity state $C(t)$ that parameterizes the feasible manifold $\Omega(u)$ and thus the congestion boundary $\partial\Omega$ (Beckmann et al., 1956; Arnott et al., 1993; Whitt, 2002; Gross et al., 2008).

The numerical goal is to demonstrate a sharp distinction between (i) a regime in which decentralized incentives expand capacity reactively, allowing congestion to bind and amplify shocks, and (ii) a regime in which a state-like controller expands capacity preemptively to keep the system below a stability boundary.

5.2. State variables and the spectral–congestion stability index

At each time step, the simulation computes two objects that jointly determine whether growth dynamics remain in a stable high-throughput corridor:

(i) Network amplification via spectral radius.
Let $A(t) \in \mathbb{R}_{+}^{N\times N}$ be the weighted directed adjacency matrix. We define the instantaneous amplification factor as the spectral radius

$$\lambda(t) = \lambda_{\max}\big(A(t)\big),$$

which captures the potential for micro shocks to propagate through interdependencies (Acemoglu et al., 2012; Gabaix, 2011; Baqaee & Farhi, 2020; Newman, 2003; Barabási, 2016).

(ii) Capacity geometry via a diverging congestion potential.
Capacity constraints are implemented by a congestion potential $\Phi(Q, C)$ that diverges as $Q(t) \uparrow C(t)$. Consistent with queueing and bottleneck congestion stylizations (Beckmann et al., 1956; Arnott et al., 1993; Whitt, 2002), we use

$$\Phi(Q, C) = \frac{Q}{C - Q}, Q < C,$$

and define a smooth attenuation factor

$$\Xi(C, Q) = \exp\{-\beta\, \Phi(Q, C)\},$$

so that congestion collapses effective propagation capacity as throughput approaches the boundary $\partial\Omega$.

Effective amplification index.

We then define the key composite diagnostic:

$$R(t) \;=\; \lambda(t)\,\Xi\big(C(t), Q(t)\big).$$

The interpretation is operational: $\lambda(t)$ measures **network fragility / propagation power**, while $\Xi(C, Q)$ measures capacity feasibility. The product $R(t)$ is therefore an effective amplification index that becomes large when the network is tightly coupled *and* operating close to capacity, precisely the configuration in which small shocks induce macro volatility.

We mark the stability boundary as

$$R(t) \leq 1,$$

which plays the role of a computational "no-crisis corridor": once $R(t)$ crosses below unity, the combination of network coupling and congestion is sufficiently damped that shock propagation is controlled (conceptually aligned with resilience thresholds in complex networks; Gao et al., 2016).

5.3. Regimes, policy proxy, and finite-horizon transitional setting

We implement a finite-horizon transitional problem over $T = 10$ (years, normalized time units) with Euler–Maruyama discretization step $dt = 0.02$, consistent with computational SDE practice in economics and control (Judd, 1998; Fleming & Soner, 2006). The simulation compares two regimes:

Regime A (decentralized/reactive capacity expansion).

Infrastructure investment is activated only when throughput is already close to the capacity boundary; this mimics delayed private response to long-horizon public goods and coordination failures.

Regime B (endogenous stabilization / anticipatory expansion).

The controller invests as a function of the stability risk signal $R(t)$, expanding capacity *before* bottlenecks bind; this is the finite-horizon analogue of a stabilization policy that is consistent with dynamic control logic (Bellman, 1957; Fleming & Soner, 2006) and compatible with the paper's differential-game framing (Başar & Olsder, 1999; Friedman, 1971).

While the present section uses a policy proxy (a monotone investment response to $R(t)$) to keep the computation transparent, it is structurally consistent with the HJB logic developed earlier: reactive policy is dominated in stochastic environments, because the congestion penalty is convex/diverging near the boundary.

5.4. Emergent order parameter and phase-transition interpretation

To express "middle-income trap" dynamics as a computable phase transition, we define a macro order parameter as a smooth functional of the stability index:

$$\Psi(t) = \sigma(\kappa\,[1 - R(t)]) \in (0,1),$$

where $\sigma(\cdot)$ is the logistic map and $\kappa > 0$ is a steepness parameter. Under this definition:

- $\Psi(t) \approx 0$ corresponds to an unstable, congestion-bound, high-amplification regime (trap-like dynamics).
- $\Psi(t) \to 1$ corresponds to a stabilized, decongested regime where network propagation is damped and the system can support persistent throughput expansion.

This construction mirrors statistical-mechanics practice: instead of imposing a transition exogenously, we compute an order parameter from an internally defined control/stability functional, allowing the phase change to be observed in simulation rather than assumed (Bouchaud, 2008; Chakraborti et al., 2011; Sinha et al., 2010).

5.5. Calibration and reproducibility

All parameters used in the numerical experiments are reported in Table 2, and notation is summarized in Table 1 to ensure direct reproducibility. The simulated network uses $N = 200$ nodes (reduced-form spectral simulation), horizon $T = 10$, time step $dt = 0.02$, intrinsic throughput growth coefficient $q_{\text{growth}} = 0.12$, capacity decay $\eta = 0.05$, throughput shock scale $\sigma_q = 1.2$, and adjacency shock scale $\sigma_a = 0.005$. These values are not intended as country-specific calibration; they are chosen to produce a stable numerical integration and to clearly separate the qualitative regimes induced by reactive versus anticipatory capacity expansion.

5.6. Visual diagnostics and conceptual scaffolding

Figures 1–3 are included as interpretive scaffolding that links the simulation objects to the theory:

- The directed bipartite topology (Figure 1) clarifies the conceptual separation between policy-linked nodes and market nodes, consistent with the bipartite modeling strategy common in production-network analysis (Acemoglu et al., 2012; Schweitzer et al., 2009).
- The tilted potential landscape (Figure 2) communicates the Hamiltonian intuition: stabilization changes the energy landscape so that the high-productivity basin becomes dynamically reachable.
- The capacity geometry phase portrait (Figure 3) visualizes how friction intensifies near the boundary $\partial\Omega$, consistent with queue/bottleneck nonlinearity (Beckmann et al., 1956; Arnott et al., 1993; Gross et al., 2008).

The computational results (Figures 4–6) then formalize these intuitions quantitatively through $C(t)$, $Q(t)$, $\lambda(t)$, and the stability index $R(t)$.

Table 1. Nomenclature and Variable Definition

Symbol	Definition
U	Policy-linked node set
V	Market-oriented node set
$A(t)$	Weighted directed adjacency matrix
$\big(\lambda(t)\big)$	Spectral radius of $(A(t))$
$\big(C(t)\big)$	Infrastructure capacity state
$\big(Q(t)\big)$	Aggregate throughput state
$\big(\Phi(Q,u)\big)$	Congestion potential (diverging at boundary)

Symbol	Definition
$\left(\Xi(C,Q)\right)$	Congestion attenuation factor
$\left(R(t)\right)$	Effective amplification index $\lambda(t) \cdot \Xi\left(C(t),Q(t)\right)$
$\left(\Psi(t)\right)$	Order parameter derived from $\left(R(t)\right)$

Table 2. Simulation Parameters

Parameter	Value	Description
N	200	Nodes used for spectral simulation (reduced form)
T	10	Finite transition horizon
dt	0.02	Euler–Maruyama time step
q_{growth}	0.12	Intrinsic throughput growth coefficient
η	0.05	Capacity decay
σ_q	1.2	Throughput shock scale
σ_a	0.005	Adjacency shock scale

Figure 1: Directed Bipartite Production Network (Conceptual)

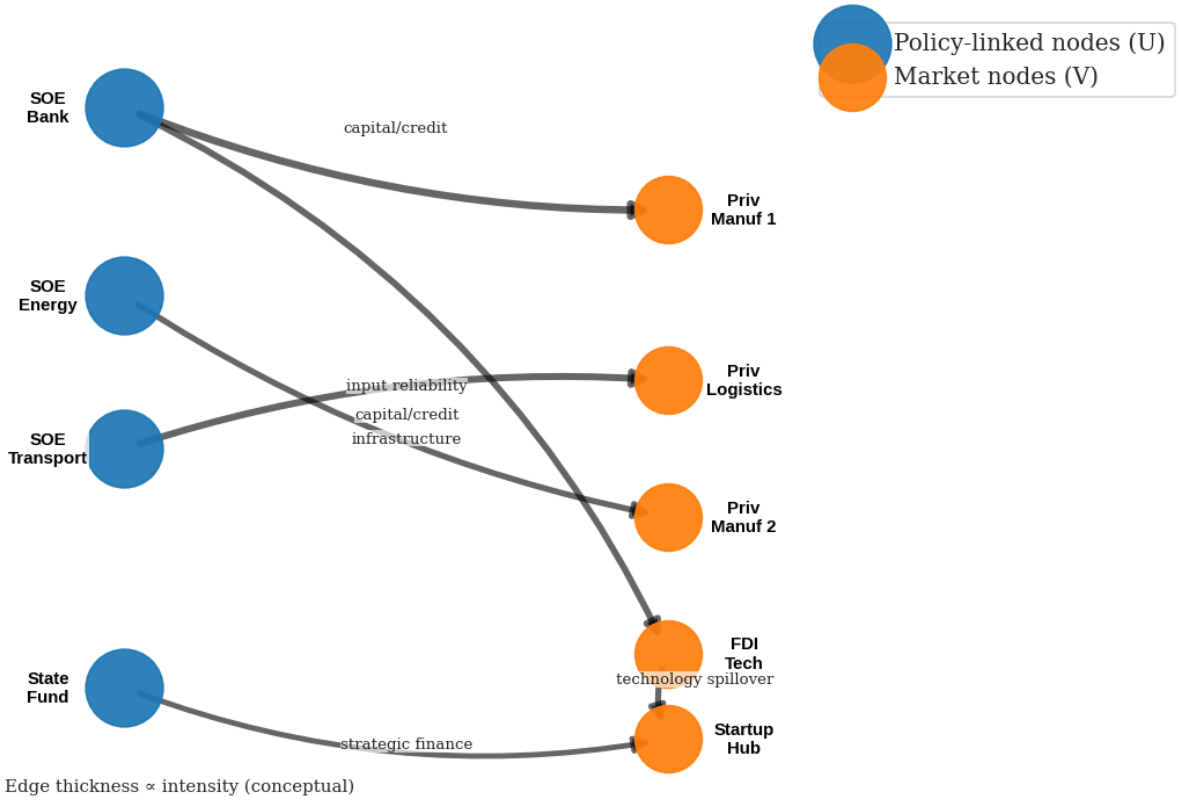


Figure 1 | Bipartite Production Network. Contrast between policy-linked (State) and market-oriented (Private) actors. Uses a weighted directed adjacency matrix $A(t)$.

Figure 2: Potential Landscape with Stabilization Tilt (Conceptual)

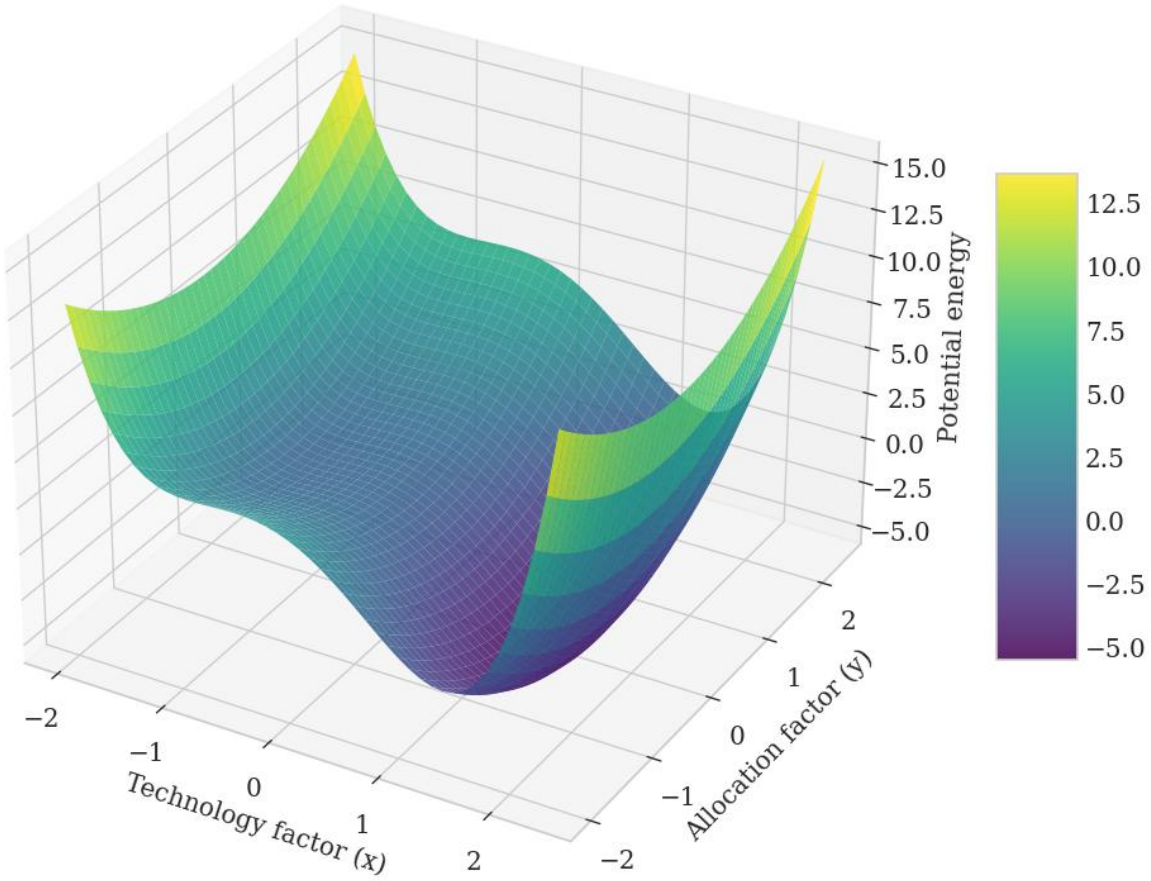


Figure 2 | Potential Landscape. A double-well potential. Policy acts as a "tilt" to push the system out of a low-productivity trap.

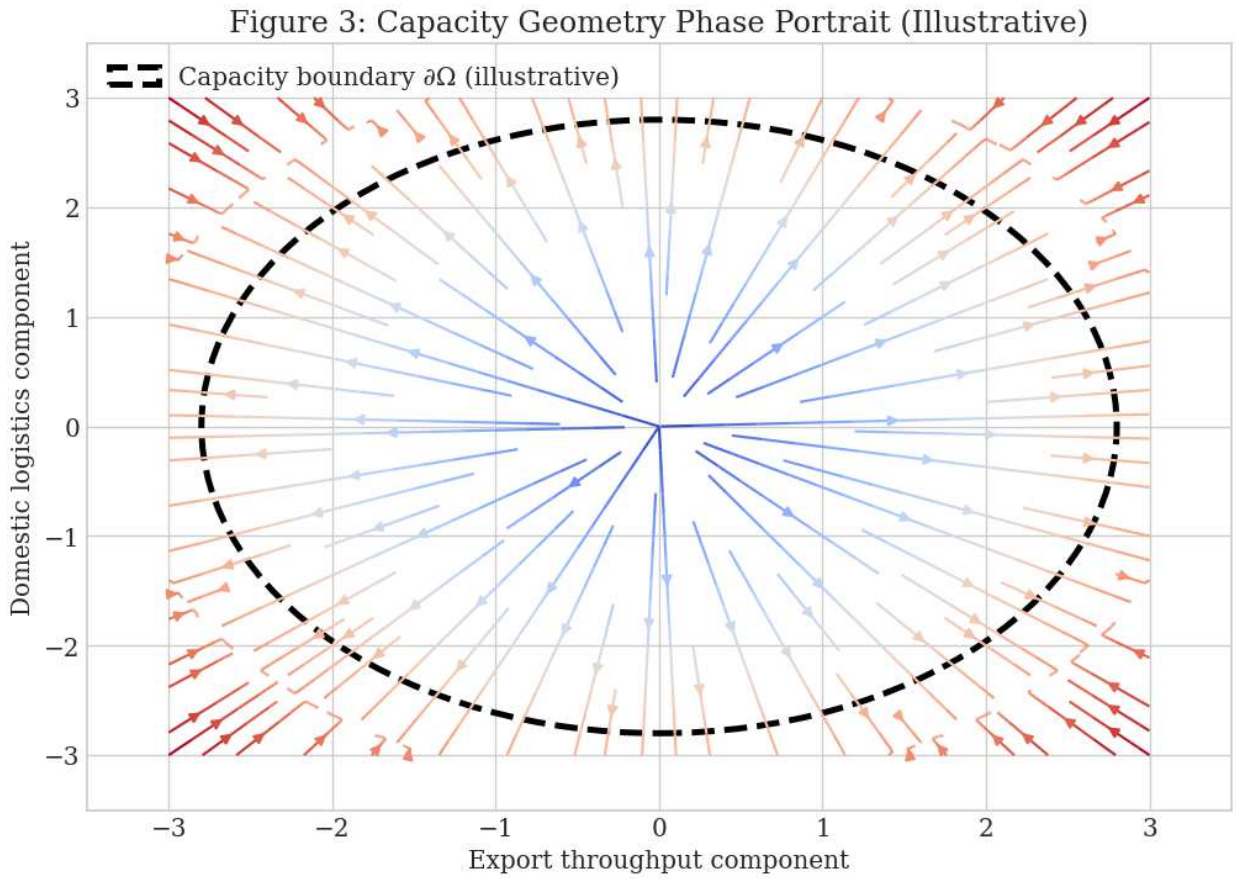


Figure 3 | Capacity Geometry. Phase portrait showing growth pressure vs. capacity limits. Highlights "nonlinear friction" (congestion) as throughput Q nears capacity C.

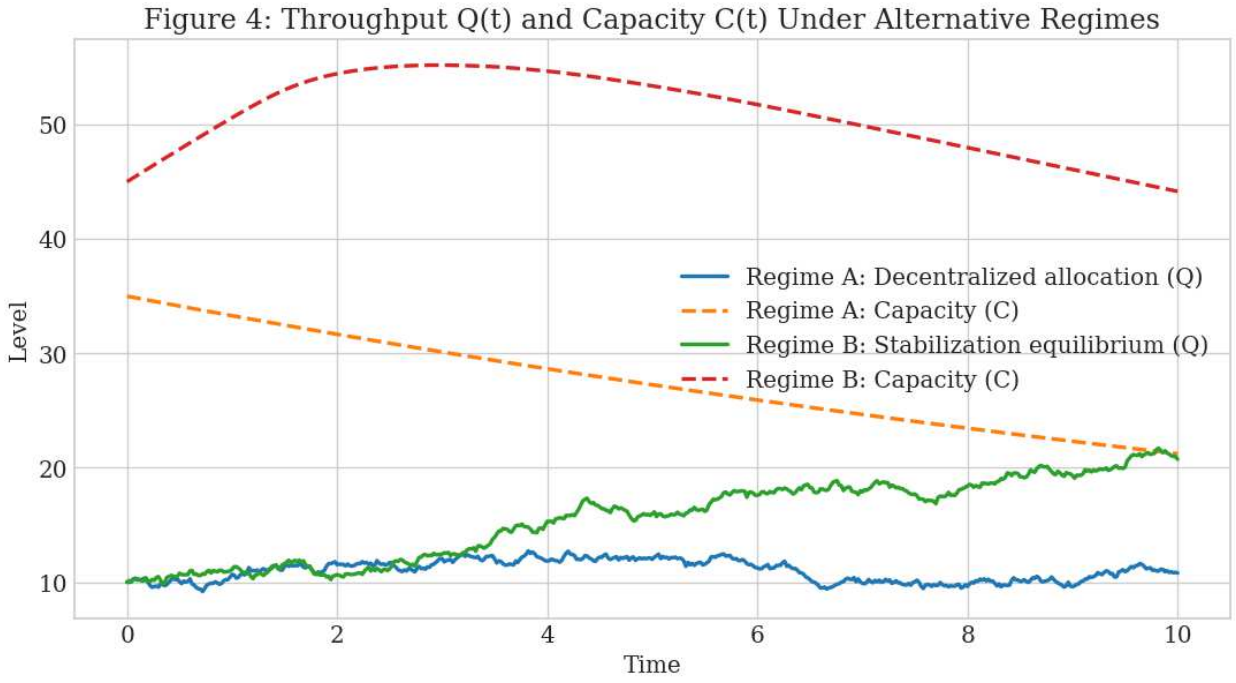


Figure 4 | Throughput (Q) vs. Capacity (C). Compares Regime A (reactive capacity growth) vs. Regime B (preemptive growth).

5.7. Results: stabilization boundary and resilience contrast

Figure 5 reports the evolution of the effective amplification index $R(t) = \lambda(t)\Xi(C, Q)$ under the two regimes, with the stabilization boundary $R = 1$ shown explicitly. The results exhibit a sharp contrast:

- Under **Regime B**, $R(t)$ collapses below unity early (approximately by $t \approx 2$ in the rendered output), indicating that anticipatory capacity expansion rapidly increases $\Xi(C, Q)$ and thus neutralizes the amplification channel even when the adjacency structure remains nontrivial.
- Under **Regime A**, $R(t)$ declines much more slowly, crossing the boundary only later (approximately $t \approx 4$–5). This delay corresponds to the model's congestion logic: reactive expansion allows $Q(t)$ to approach $C(t)$, driving $\Phi(Q, C)$ upward and suppressing effective flow only after instability has already emerged.

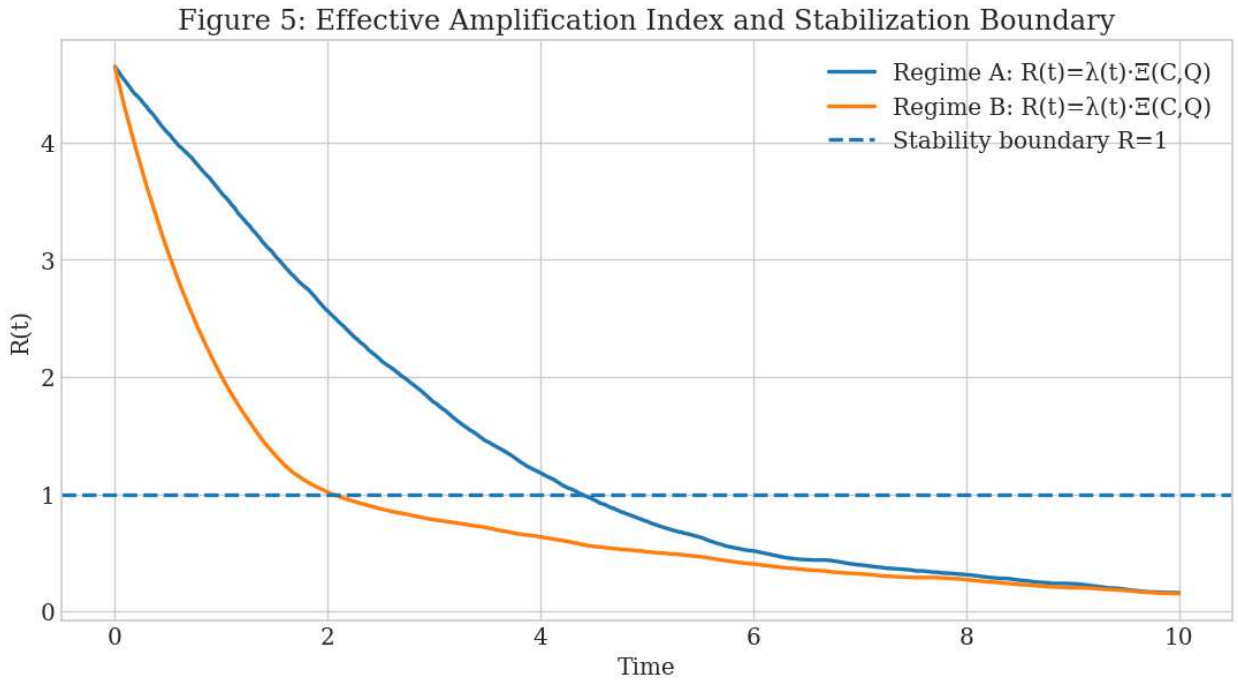


Figure 5 | Amplification Index (R). Tracks the stability diagnostic $R(t) = \lambda(t)\Xi\big(C(t), Q(t)\big)$. Crossing $R = 1$ signifies system stabilization.

Figure 6 translates this stability story into the macro phase-transition language: $\Psi(t)$ increases earlier and more smoothly under the stabilization regime, while the decentralized regime lags substantially. Importantly, $\Psi(t)$ is **not imposed**; it is computed from $R(t)$. Thus, the "escape" trajectory is emergent: as capacity expansion keeps the system away from $\partial\Omega$, attenuation improves and the effective amplification falls, pushing $\Psi(t) \to 1$.

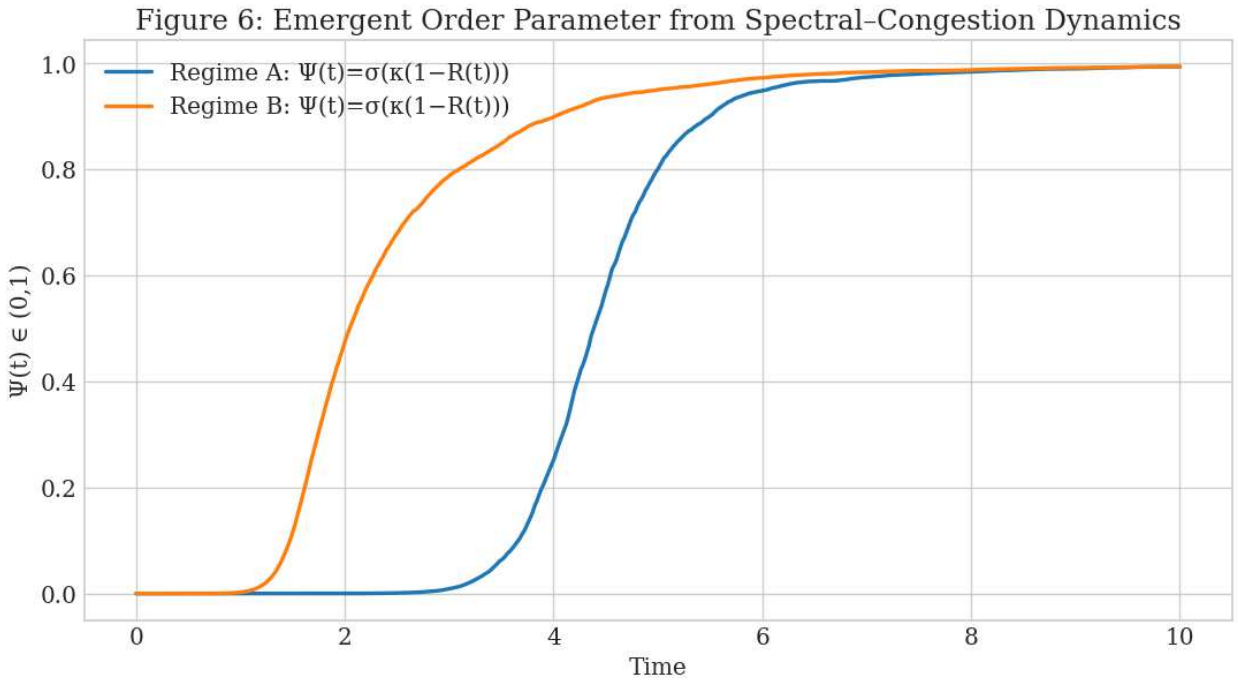


Figure 6 | Order Parameter (Ψ). The final macro-indicator $\Psi(t) \in (0,1)$ showing how quickly the system reaches a stabilized path.

Taken together, the simulated evidence supports the paper's central claim: **endogenous stabilization operates by preemptively expanding feasible capacity geometry**, which changes the spectral–congestion regime of the production network and prevents congestion-amplified volatility from becoming the default "market-clearing" adjustment mechanism.

5.8. Discussion: why preemption dominates reaction under stochastic transport

The decisive mechanism is convexity/divergence: because $\Phi(Q, C)$ increases sharply as $Q \uparrow C$, the marginal benefit of capacity expansion is highest before the system is congestion-bound. In stochastic environments, waiting for bottlenecks to appear is mathematically dominated: random shocks push $Q(t)$ toward the boundary, and once near $\partial\Omega$, congestion induces a regime where effective damping collapses and network propagation dominates. This is precisely why the anticipatory regime rapidly forces $R(t)$ below unity, while the reactive regime remains exposed to prolonged instability. The simulation therefore operationalizes the paper's thesis: escaping the middle-income trap is a stability-control problem in a directed economic network with capacity geometry, not a purely factor-accumulation story (Solow, 1956; Aghion & Howitt, 1992; Acemoglu et al., 2006; Rodrik, 2016; Stiglitz, 1996).

6. Structural Policy Implications: Engineering Transitional Stability

The theoretical and computational results establish that transitional growth in directed production networks is governed by the stability condition

$$R(t) = \lambda(t)\,\Xi(C(t), Q(t)) \leq 1,$$

where $\lambda(t)$ captures network amplification and $\Xi(C, Q)$ captures congestion attenuation derived from capacity geometry.

Table 3 summarizes the structural policy levers implied by the model and their precise impact on this stability condition.

Table 3 | Structural policy levers and their effects on network stability. *Each lever is interpreted through its impact on the effective amplification index* $R(t) = \lambda(t)\Xi(C, Q)$.

Policy Lever	Primary Model Channel	Effect on Stability Index	Transitional Impact
Preemptive infrastructure expansion	Increases $C(t)$, raises $\Xi(C, Q)$	Reduces $R(t)$ via stronger attenuation	Shortens time to $\Psi(t) \to 1$
Strategic capital routing	Moderates growth of $\lambda(t)$; reshapes $A(t)$	Reduces propagation intensity	Limits amplification-dominated regime
Shock-absorbing central nodes	Dampens volatility of $A(t)$	Reduces variance of $\lambda(t)$	Smooths transitional path

Policy Lever	Primary Model Channel	Effect on Stability Index	Transitional Impact
Innovation-directed liquidity	Expands productive frontier capacity	Raises sustainable $C(t)$ trajectory	Supports high-TFP equilibrium

The objective of policy in transitional economies is therefore not merely to increase capital inflows or deregulate markets, but to manage the joint evolution of:

- Network propagation intensity ($\lambda(t)$),
- Infrastructure capacity ($C(t)$),
- Throughput proximity to the boundary ($Q(t) \to C(t)$).

Figure 7: Structural Policy Channels and Stability Mechanism

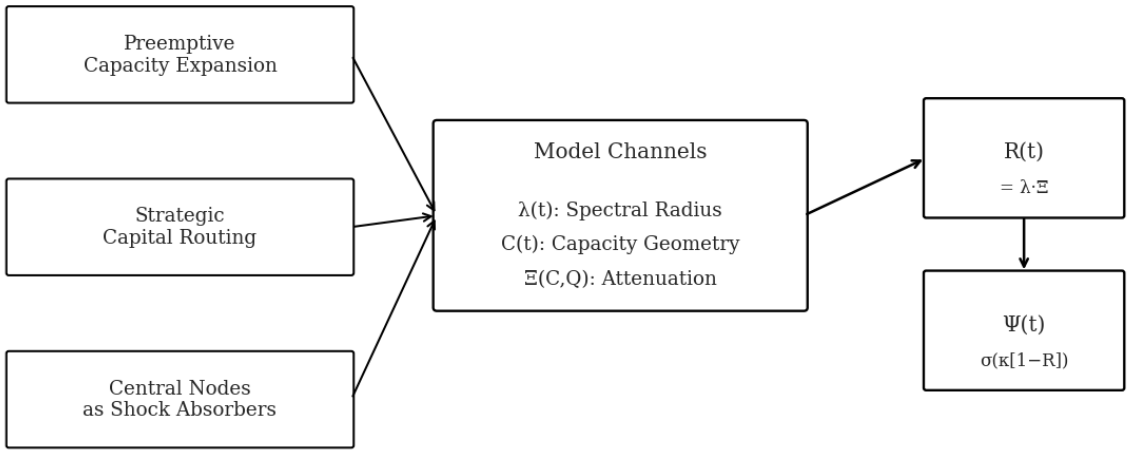


Figure 7 | Structural policy channels and stability mechanism. Policy levers influence the effective amplification index $R(t) = \lambda(t)\Xi\big(C(t), Q(t)\big)$ through their impact on network

propagation intensity $\lambda(t)$ and capacity geometry $C(t)$. The attenuation factor $\Xi(C, Q)$ links congestion to amplification. The macroeconomic order parameter $\Psi(t) = \sigma(\kappa[1 - R(t)])$ summarizes the transition from amplification-dominated to attenuation-dominated regimes.

6.1 Preemptive Capacity Expansion

Because the congestion potential diverges as $Q \uparrow C$,

$$\Phi(Q, C) \to \infty,$$

the attenuation factor $\Xi(C, Q)$ collapses sharply near the boundary. In stochastic environments, reactive adjustment permits throughput shocks to push the system into an amplification-dominated regime ($R(t) > 1$).

The simulations demonstrate that anticipatory expansion of $C(t)$:

- Raises $\Xi(C, Q)$,
- Reduces $R(t)$ earlier,
- Accelerates convergence of the order parameter $\Psi(t) \to 1$.

Infrastructure therefore functions as a structural stabilizer rather than a passive consequence of growth.

6.2 Capital Routing and Network Geometry

The Hamiltonian formulation implies that capital allocation reshapes the adjacency matrix $A(t)$. If financial flows disproportionately increase interdependence without parallel expansion of $C(t)$, the spectral radius $\lambda(t)$ rises faster than attenuation improves.

This produces:

$$\frac{d\lambda}{dt} > \frac{d\Xi}{dt},$$

implying $R(t) \uparrow$.

Strategic capital routing—toward productivity-enhancing sectors and infrastructure—moderates the growth of $\lambda(t)$ while supporting long-run capacity expansion. The stability gain arises from reducing propagation intensity relative to congestion attenuation.

6.3 Systemically Central Nodes as Volatility Dampeners

In network systems, large or central nodes disproportionately affect spectral properties (Gabaix, 2011). When such nodes internalize high-risk transitional investments, adjacency volatility declines.

Formally, dampening fluctuations in $A(t)$ reduces variance in $\lambda(t)$, thereby lowering the probability that $R(t)$ temporarily exceeds unity due to stochastic shocks.

The structural insight is that transitional stability improves when systemically central actors absorb high-variance adjustments rather than propagating them.

6.4 Reinterpreting the Middle-Income Trap

Under this framework, a middle-income plateau corresponds to a persistent regime where

$$\lambda(t)\,\Xi(C(t), Q(t)) > 1.$$

This may arise when integration deepens network interdependence without proportional expansion of capacity geometry.

Escaping the trap requires shifting into an attenuation-dominated regime:

$$R(t) \leq 1,$$

which corresponds to the observed rise of the order parameter $\Psi(t)$in the simulations.

Thus, transitional upgrading is a stability phase shift, not merely a capital accumulation process.

6.5 Institutional Interpretation

The model does not depend on a specific political regime. However, it implies that systems capable of synchronizing:

- Infrastructure expansion,
- Financial routing,

- Network deepening,

under a coherent long-horizon strategy are more likely to maintain $R(t) \leq 1$ throughout the transition.

The structural advantage arises from solving a stochastic optimal control problem that jointly governs adjacency evolution and capacity geometry.

Disclosure

Proclamation regarding generative AI and AI-enhanced technology in the writing process

In the course of preparing this work, the author utilized ChatGPT (OpenAI) and Gemini were used for editing and structural refinement. The author takes full responsibility for the scientific content.

References

Acemoglu, D., Aghion, P., Zilibotti, F. (2006). Distance to frontier, selection, and economic growth. Journal of the European Economic Association, 4(1), 37–74.

Acemoglu, D., Carvalho, V. M., Ozdaglar, A., Tahbaz-Salehi, A. (2012). The network origins of aggregate fluctuations. Econometrica, 80(5), 1977–2016.

Aghion, P., Howitt, P. (1992). A model of growth through creative destruction. Econometrica, 60(2), 323–351.

Arnott, R., de Palma, A., Lindsey, R. (1993). A structural model of peak-period congestion. American Economic Review, 83(1), 161–179.

Baqaee, D. R., Farhi, E. (2020). The macroeconomic impact of microeconomic shocks: Beyond Hulten's theorem. Econometrica, 88(4), 1437–1473.

Başar, T., & Olsder, G. J. (1999). Dynamic Noncooperative Game Theory. SIAM.

Barabási, A. L. (2016). Network Science. Cambridge University Press.

Beckmann, M., McGuire, C., Winsten, C. (1956). Studies in the Economics of Transportation. Yale University Press.

Bellman, R. (1957). Dynamic Programming. Princeton University Press.

Bouchaud, J.-P., & Potters, M. (2003). Theory of Financial Risk. Cambridge University Press.

Bouchaud, J. P. (2008). Economics needs a scientific revolution. Nature, 455(7217), 1181–1181.

Chakraborti, A., Toke, I. M., Patriarca, M., & Abergel, F. (2011). Econophysics review: I. Empirical facts. Quantitative Finance, 11(7), 991–1012.

Fleming, W., Soner, H. M. (2006). Controlled Markov Processes and Viscosity Solutions. Springer.

Friedman, A. (1971). Differential Games. Wiley.

Fudenberg, D., Tirole, J. (1991). Game Theory. MIT Press.

Gabaix, X. (2011). The granular origins of aggregate fluctuations. Econometrica, 79(3), 733–772.

Gao, J., Barzel, B., & Barabási, A. L. (2016). Universal resilience patterns in complex networks. Nature, 530(7590), 307–312.

Gross, D., Shortle, J. F., Thompson, J. M., & Harris, C. M. (2008). Fundamentals of Queueing Theory. John Wiley & Sons.

Hidalgo, C. A., Hausmann, R. (2009). The building blocks of economic complexity. Proceedings of the National Academy of Sciences, 106(26), 10570–10575.

Judd, K. (1998). Numerical Methods in Economics. MIT Press.

Lasry, J.-M., Lions, P.-L. (2007). Mean field games. Japanese Journal of Mathematics, 2, 229–260.

Lucas, R. E., Stokey, N. L. (1989). Recursive Methods in Economic Dynamics. Harvard University Press.

Mantegna, R. N., Stanley, H. E. (1999). An Introduction to Econophysics: Correlations and Complexity in Finance. Cambridge University Press.

Newman, M. E. J. (2003). The structure and function of complex networks. SIAM Review, 45(2), 167–256.

Pinedo, M. L. (2012). Scheduling: Theory, Algorithms, and Systems. Springer.

Rodrik, D. (2016). Premature deindustrialization. Journal of Economic Growth, 21, 1–33.

Sargent, T., Stachurski, J. (2013). Quantitative Economics with Python. MIT Press.

Schweitzer, F., Fagiolo, G., Sornette, D., Vega-Redondo, F., Vespignani, A., White, D. R. (2009). Economic networks: The new challenges. Science, 325(5939), 422–425.

Sinha, S., Chatterjee, A., Chakraborti, A., Chakrabarti, B. K. (2010). Econophysics: An Introduction. John Wiley & Sons

Solow, R. (1956). A contribution to the theory of economic growth. Quarterly Journal of Economics, 70(1), 65–94.

Sornette, D. (2014). Physics of Financial Markets. Springer.

Stiglitz, J. E. (1996). Some lessons from the East Asian Miracle. The World Bank Research Observer, 11(2), 151–177.

Whitt, W. (2002). Stochastic-Process Limits. Springer.